



## Structural basis of the selectivity of the $\beta_2$ -adrenergic receptor for fluorinated catecholamines

Chaya Pooput<sup>a</sup>, Erica Rosemond<sup>a</sup>, Joel Karpiak<sup>b</sup>, Francesca Deflorian<sup>b</sup>, Santiago Vilar<sup>b</sup>, Stefano Costanzi<sup>b</sup>, Jürgen Wess<sup>a</sup>, Kenneth L. Kirk<sup>a,\*</sup>

<sup>a</sup>Laboratory of Bioorganic Chemistry, National Institute of Diabetes and Digestive and Kidney Diseases, National Institutes of Health, DHHS, Bethesda, MD 20892, USA

<sup>b</sup>Laboratory of Biological Modeling, National Institute of Diabetes and Digestive and Kidney Diseases, National Institutes of Health, DHHS, Bethesda, MD 20892, USA

### ARTICLE INFO

#### Article history:

Received 11 August 2009

Revised 6 October 2009

Accepted 7 October 2009

Available online 13 October 2009

#### Keywords:

G protein-coupled receptors

Adrenergic agonists

Fluorine substitution

Catecholamines

Receptor selectivities

Point mutations

Receptor modeling

### ABSTRACT

The important and diverse biological functions of adrenergic receptors, a subclass of G protein-coupled receptors (GPCRs), have made the search for compounds that selectively stimulate or inhibit the activity of different adrenergic receptor subtypes an important area of medicinal chemistry. We previously synthesized 2-, 5-, and 6-fluoronorepinephrine (FNE) and 2-, 5-, and 6-fluoroepinephrine (FEPI) and found that 2FNE and 2FEPI were selective  $\beta$ -adrenergic agonists and that 6FNE and 6FEPI were selective  $\alpha$ -adrenergic agonists, while 5FNE and 5FEPI were unselective. Agonist potencies correlated well with receptor binding affinities. Here, through a combination of molecular modeling and site-directed mutagenesis, we have identified N293 in the  $\beta_2$ -adrenergic receptor as a crucial residue for the selectivity of the receptor for catecholamines fluorinated at different positions.

Published by Elsevier Ltd.

### 1. Introduction

Norepinephrine (NE) (**1a**) is the principal neurotransmitter of the sympathetic nervous system, and both NE and epinephrine (EPI) are important neurotransmitters in the central nervous system. In addition, EPI (**1b**) is the principal hormone of the adrenal medulla. These catecholamine ligands regulate the activity of most peripheral organs and tissues including blood vessels, heart, liver, lungs, and smooth muscle. In the central nervous system, NE and EPI are involved in many important functions, such as learning, memory and sleep–wake cycle regulation, and behavioral processes.<sup>1</sup>

The biological effects of NE and EPI are mediated through the interaction with adrenergic receptors, members of the superfamily of G protein-coupled receptors (GPCRs). These membrane-associated receptors possess seven transmembrane domains (TM 1–7) connected by three intra- and three extracellular loops. Molecular cloning studies have revealed the existence of nine adrenergic receptor subtypes, including three  $\alpha_1$  ( $\alpha_{1a}$ ,  $\alpha_{1b}$ , and  $\alpha_{1d}$ ), three  $\alpha_2$  ( $\alpha_{2a}$ ,  $\alpha_{2b}$ , and  $\alpha_{2c}$ ), and three  $\beta$  ( $\beta_1$ ,  $\beta_2$ , and  $\beta_3$ ) receptors.<sup>2,3</sup>

The important and diverse biological functions of the different adrenergic receptor subtypes have made the search for compounds that selectively stimulate or inhibit the activity of each individual

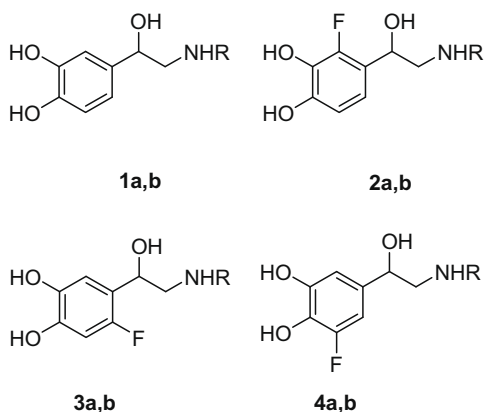
receptor subtype an important area of medicinal chemistry. We discovered several years ago that fluorine substitution on the aromatic ring of NE, EPI, and related adrenergic agonists dramatically alters the selectivity of these agonists for  $\alpha$ - and  $\beta$ -adrenergic receptors, depending on the site of substitution.<sup>4,5</sup> The 2-fluoro analogues (**2a,b**) bind selectively to the  $\beta_2$ -adrenergic receptor while the 6-fluoro analogues (**3a,b**) bind preferentially to the  $\alpha_{1b}$ -adrenergic receptor. In contrast, the 5-fluoro-analogues (**4a,b**) did not display selectivity for  $\alpha$ - or  $\beta$ -adrenergic receptors and had similar potency to the parent compounds. Examination of the effect of fluorine at each available position of an aromatic ring on biological activity is currently termed a ‘fluorine scan’.<sup>6</sup>

The  $\alpha$ - and  $\beta$ -selective fluorinated analogues of NE and EPI proved to be valuable pharmacological agents, in part because of the close structural similarity of these analogues to the natural compounds.<sup>7</sup> In addition to pharmacological studies, we also carried out extensive research designed to determine the molecular mechanism(s) underlying these fluorine-induced selectivities. Several intra- and inter-molecular mechanisms were proposed to explain the ‘anti-symmetric’ nature of the selectivity. For example, intramolecular hydrogen bonding between the benzylic OH group and an *ortho*-fluorine substituent,<sup>4</sup> or dipole–dipole repulsions between the COH and CF bonds<sup>8</sup> were considered as factors which could lead to predominant conformations favorable for binding to  $\alpha$ - or  $\beta$ -adrenergic receptors. Alternatively, it has been proposed

\* Corresponding author. Tel.: +1 301 496 2619; fax: +1 301 402 4182.

E-mail address: [kennethk@bdg8.niddk.nih.gov](mailto:kennethk@bdg8.niddk.nih.gov) (K.L. Kirk).

Series a: R = H  
Series b: R = Me



that fluorine-induced alterations in the electron density distributions of the catechol ring could lead to differential inhibition of binding to  $\alpha$ - or  $\beta$ -adrenergic receptors.<sup>9,10</sup> Attempts were made to examine the effects of intramolecular interactions by synthesizing several structural analogues of the fluorinated catecholamines wherein such interactions, if they existed, would be expected to be quite different.<sup>7–12</sup> These early studies were carried out using membrane tissues known to possess, predominantly, single adrenergic receptor subtypes. Unfortunately, the results of these studies were inconclusive.

Since structural modifications of the fluorinated agonists led to no clear answer as to the mechanism by which fluorine induces selectivity for certain adrenergic receptor subtypes, we have turned our attention to modifications of the structure of the receptor itself as a strategy to solve this problem. In this report we describe our efforts to localize the region on the receptor which discriminates between 2-F and 6-F substitution of catecholamines by studying various mutant receptors. Specific amino acids were targeted by site-directed mutagenesis, guided by molecular modeling studies.

Since the X-ray structure of the  $\beta_2$ -adrenergic receptor had not been published at the start of this study, we initially generated a rhodopsin-based homology model of the  $\beta_2$  receptor, as described elsewhere.<sup>13</sup> On the basis of this model, for which a subsequent comparison with the later published crystal structure revealed a substantial accuracy,<sup>13</sup> we located the residues that line the NE binding pocket according to a binding mode considered well established in the literature,<sup>14–18</sup> and by means of sequence comparison identified slight differences with the corresponding residues in the

$\alpha_{1b}$  subtype that conceivably could be responsible for the selectivity of the fluorinated catecholamines. Guided by these considerations, site-directed mutagenesis was used to target these amino acids. Using radioligand binding assays, the effects of the various mutations on the binding of 2FNE and 6FNE were probed. Based on observed alterations in binding of the fluorinated analogues, second generation mutants were constructed and studied. Our goal was to identify point mutations that were able to reverse the preference of the  $\beta_2$ -adrenergic receptor for the 2FNE versus the 6FNE. While this study was ongoing, the crystal structure of the human  $\beta_2$ -adrenergic receptor was published,<sup>19,20</sup> providing us with a more solid experimental platform upon which to base the last stage of our modeling. In particular, we used the new crystal structure and a model of the N293F mutant receptor based on this structure to computationally dock 2FNE and 6FNE, in order to understand the molecular basis underlying the selectivity of the  $\beta_2$ -adrenergic receptor toward 2FNE.

## 2. Results and discussion

As part of our research on the adrenergic receptor subtype selectivities of 2FNE and 6FNE (as well as of fluorinated analogues of related adrenergic agonists), agonist potencies were found to correlate with relative receptor binding affinities to the receptors.<sup>4</sup> In previous studies, competition binding assays were carried out using rat cerebral cortical membranes using radioligands selective for  $\alpha_1$ -,  $\alpha_2$ -,  $\beta_1$ -, and  $\beta_2$ -adrenergic receptors.<sup>12,21</sup> In the present investigation, we initially confirmed these findings using recombinant human  $\alpha_{1b}$ - and  $\beta_2$ -adrenergic receptor subtypes transiently expressed in mammalian COS7 cells. [<sup>3</sup>H]-Prazosin and [<sup>3</sup>H]-dihydroalprenolol (DHA) were used as selective radioligands for the  $\alpha_{1b}$ - and  $\beta_2$ -adrenergic receptors, respectively. Our results were consistent with previous findings using rat membranes, in that 6FNE had a higher affinity than 2FNE at the  $\alpha_{1b}$ -adrenergic receptor (6FNE  $K_i = 4.0 \pm 0.9 \mu\text{M}$ ; 2FNE  $K_i = 134 \pm 5 \mu\text{M}$ ) and 2FNE had higher affinity than 6FNE at the  $\beta_2$ -adrenergic receptor (2FNE  $K_i = 16 \pm 0.8 \mu\text{M}$ ; 6FNE  $K_i = 1160 \pm 51 \mu\text{M}$ ) (Table 1).

A rhodopsin-based homology model of the  $\beta_2$ -adrenergic receptor, the construction of which is described elsewhere,<sup>13</sup> was used to identify the residues lining the orthosteric binding site according to the NE binding mode well established in the literature (Fig. 1).<sup>14–18</sup> In particular, we focused on the cavity located within the portion of the helical bundle of the receptor that faces the extracellular side, and is lined on one side by D113 in TM3 and on the other side by three TM5 serine residues (S203, S204, and S207). A sequence comparison showed differences in the binding pocket residues detected in our  $\beta_2$ -adrenergic receptor model and the corresponding residues in the  $\alpha_{1b}$  subtype. In particular,

**Table 1**  
Binding affinities ( $K_i$  values) of NE, 2FNE, and 6FNE towards wild type and mutant  $\beta_2$ -adrenergic receptors<sup>a</sup>

	$K_d$ (nM) <sup>b</sup>	NE		2FNE		6FNE	
		$K_i$ ( $\mu\text{M}$ )	$\Delta K_i^c$	$K_i$ ( $\mu\text{M}$ )	$\Delta K_i^c$	$K_i$ ( $\mu\text{M}$ )	$\Delta K_i^c$
$\alpha_{1b}$	$0.80 \pm 0.11$	$20.4 \pm 0.5$		$134 \pm 4.9$		$4.0 \pm 0.9$	
$\beta_2$	$0.69 \pm 0.20$	$96.7 \pm 1.5$		$15.8 \pm 8.4$		$1160 \pm 51$	
V117C	$1.23 \pm 0.15$	$217 \pm 18.2$	+2.1	$39.8 \pm 6.4$	+2.5	>2000	
T164I	$2.38 \pm 0.13$	$191 \pm 9.3$	+1.9	$38.7 \pm 21.8$	+2.4	>2000	
D192G, F193V	$1.60 \pm 0.14$	$134 \pm 43.5$	+1.4	$19.5 \pm 0.4$	+1.2	>2000	
N293L	$0.88 \pm 0.03$	$378 \pm 78.6$	+3.9	$117 \pm 1$	+7.4	$188 \pm 0.8$	−6.0
N293A	$0.79 \pm 0.07$	$1776 \pm 33.0$	+18.4	$319 \pm 59$	+20.2	$5446 \pm 134$	+4.7
N293Q	$1.73 \pm 0.14$	$342 \pm 59$	+3.5	$68.9 \pm 3.2$	+4.3	$3326 \pm 58.3$	+2.9
N293F	$0.95 \pm 0.12$	$490 \pm 66$	+5.1	$216 \pm 14$	+13.5	$70.1 \pm 17.7$	−16.5

<sup>a</sup> All binding studies were carried out with membranes prepared from transiently transfected COS7 cells. Data are given as means  $\pm$  SEM ( $n = 3$ ).

<sup>b</sup>  $K_d$  and  $K_i$  values were determined by using [<sup>3</sup>H]-prazosin and [<sup>3</sup>H] DHA as, respectively, radioligand of  $\alpha_{1b}$ - and  $\beta_2$ -adrenergic receptors and its mutants.

<sup>c</sup> Fold increase (+) or decrease (−) of  $K_i$  values relative to that of the wild type.

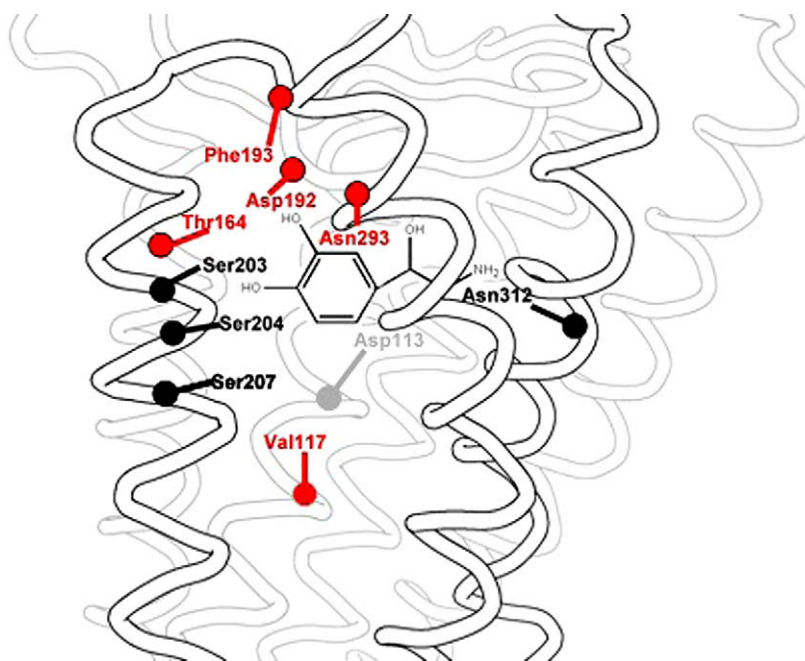


**Figure 1.** A spatial illustration of NE binding to the  $\beta_2$ -adrenergic receptor based on a homology model derived from rhodopsin. This homology model was used to design the mutagenesis experiments in the initial phase of this study, which was conducted prior to the publication of the crystal structure. Notably, a comparison with the subsequently published crystal structure revealed a substantial accuracy of our rhodopsin-based model, arguing in favor of its applicability to drug discovery.<sup>13</sup> All the subsequent calculations were instead based on the actual crystal structure of the receptor. The residues highlighted in red are those that are dissimilar to the corresponding residues in the  $\alpha_{1b}$  receptor, and were subjected to mutagenesis studies. The other residues shown are known to be important for agonist binding and receptor activation. Binding pocket residues in the foreground are shown in black, and residues in the background are shown in gray.

residues C129, I176, G196, V197, and L314 on the  $\alpha_{1b}$  subtype correspond to, respectively, V117, T164, D192, F193, and N293 on the  $\beta_2$  subtype.

Based on these models, mutant receptors were constructed in which  $\beta_2$ -adrenergic receptor residues were replaced with the corresponding  $\alpha_{1b}$ -adrenergic receptor residues (V117C; T164G; D192G, F193V, N293L). Due to the lack of crystal structure of  $\alpha_{1b}$ -adrenergic receptor, we decided to focus mainly on the studies of mutants from  $\beta_2$ -adrenergic receptor, whose high-resolution crystal structure was recently published.<sup>20</sup> The wild type and mutant adrenergic receptors were transiently expressed in COS7 cells. Binding assays were carried out using [<sup>3</sup>H]-prazosin and [<sup>3</sup>H]-dihydroalprenolol (DHA) as radioligands to selectively label  $\alpha_{1b}$ - and  $\beta_2$ -adrenergic receptors, respectively (Table 1).

At most  $\beta_2$ -adrenergic receptor mutants, the binding affinities of the NE analogues were comparable to those for the wild type receptor, except for the N293L mutant receptor. This substitution, which involved replacement of the polar side chain of asparagine with the hydrophobic side chain of leucine, caused a shift in selectivity toward an  $\alpha$ -receptor-like ligand binding profile. Thus, the affinity of 2FNE for the N293L receptor was greatly decreased (>7-fold), whereas the affinity of 6FNE was significantly improved (sixfold).

Based on the ligand binding results and the promising data from N293L mutant, we decided to focus mainly on  $\beta_2$ -adrenergic receptor and designed and tested a new set of N293 mutant  $\beta_2$ -adrenergic receptors. In order to eliminate possible functional interactions between the amino acid side chain at position 293 and the fluorine substituent of the ligand, N293 was replaced with alanine. This resulted in a pronounced reduction in ligand binding affinities ( $\Delta K_i$ [NE] = +18.4,  $\Delta K_i$ [2FNE] = +20.2,  $\Delta K_i$ [6FNE] = +4.7). To explore steric factors at position 293, N293 was replaced with glutamine, which possesses a longer amino acid side chain. This mutation also resulted in a modest reduction in ligand binding affinities ( $\Delta K_i$ [NE] = +3.5,  $\Delta K_i$ [2FNE] = +4.3,  $\Delta K_i$ [6FNE] = +2.9). In contrast, the presence of

phenylalanine, a large non-polar group, in the N293F mutant receptor resulted in a reversal of selectivity with a significantly higher affinity towards 6FNE than 2FNE ( $\Delta K_i$ [2FNE] = +13.5,  $\Delta K_i$ [6FNE] = −16.5). This is in marked contrast to the wild type  $\beta_2$ -adrenergic receptor that is much more selective towards 2FNE. These results indicate the importance of the identity of the residue at position 293 in the  $\beta_2$  receptor for the binding selectivity of fluorinated catecholamines.

In order to further investigate these observations computationally, NE, 2FNE, and 6FNE were docked with GLIDE XP,<sup>22</sup> as implemented in the Schrödinger package,<sup>23</sup> at the wild type  $\beta_2$ -adrenergic receptor and the receptor containing the N293F mutation. As mentioned, the recent crystal structure of the  $\beta_2$ -adrenergic receptor was used as the basis for all docking studies.<sup>19,20</sup> As explained in the experimental section, the docking procedure produced a maximum of three poses per ligand; of these, we discarded those not consistent with the receptor–ligand interactions known from previous biochemical and biophysical experiments.<sup>14–18,24,25</sup> In particular, we required the positively charged amine and the  $\beta$ -hydroxyl group of the ligand to establish hydrogen bonds with Asp113 in TM3 and Asn312 in TM7, according to the geometry revealed by the crystal structure. The top ranking accepted poses of the three ligands within the native and mutant receptors are shown in Figure 2. In the wild type receptor, the *meta*-hydroxyl group of the ligands points towards the extracellular region of the receptor for NE (**2a**) and 2FNE (**2b**), whereas for 6FNE it points in the opposite direction (**2c**). For both of the fluorinated compounds, this results in the fluorine substituent pointing towards residue N293. N293 is also able to hydrogen bond with the hydroxyl groups of 2FNE and NE but not 6FNE, thus explaining the lower affinity of this compound.

In the N293F mutant, the binding poses of the ligands remain the same as in the wild type receptor (**2d–2f**). However, as seen in Figure 3a, the bulky phenylalanine side chain now sterically clashes with the *meta*-hydroxyl of the catechol ring of NE and



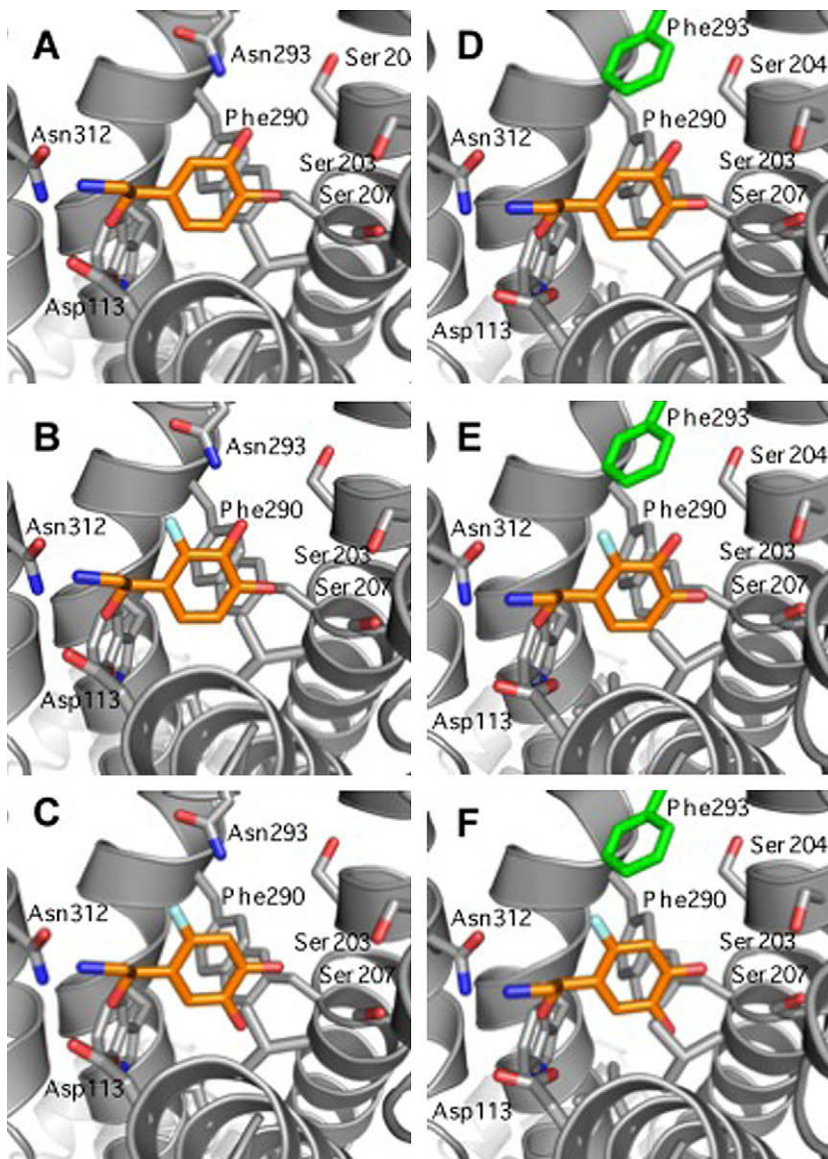


**Figure 2.** The binding modes of NE, 2FNE, and 6FNE at the wild type  $\beta_2$ -adrenergic receptor (A–C, respectively) and N293F mutant receptors (D–F). The poses for the native receptor are very similar to the poses in the N293F mutant receptor, indicating that the binding mode of the ligands does not change with the N293F mutation.

2FNE. This, along with the elimination of the hydrogen bonds present in the wild type receptor, results in the 5- and 13.5-fold loss of affinity, respectively, in the N293F mutant. On the contrary, the opposite orientation of the *meta*-hydroxyl group in 6FNE (Fig. 3b) prevents this unfavorable interaction and instead favors a newly acquired hydrophobic and  $\pi$ – $\pi$  interaction that explains the 16.5-fold increase of the affinity of this compound.

It is worth noting that also in the lower ranking accepted poses, when present, the fluorine substituent of 2FNE and 6FNE pointed towards the extracellular side of the receptor both in the wild type and in the mutant receptor, indicating its large influence in the orientation of the catechol ring.

### 3. Conclusion

Using a combined molecular modeling/site-directed mutagenesis approach, we have attempted to identify key residues in the  $\beta_2$ -adrenergic receptor that determine the binding preferences of fluorinated catecholamines, by focusing, in particular, on the contribution of residue N293 of the  $\beta_2$ -adrenergic receptor. Notably,

the design of the site-directed mutagenesis experiments was done on the basis of a rhodopsin-based homology model of the receptor, before its crystal structure became available. Thus, our identification of a residue with a profound effect on ligand recognition provides another argument in favor of the applicability of homology modeling to the study of the structure–function relationships of the GPCRs. The following part of this work was instead based on the subsequently published crystal structure of the  $\beta_2$ -adrenergic receptor. Although this structure has been obtained in complex with an inverse agonist, several studies have demonstrated that it can be effectively used to dock agonists too. In particular, docking-based virtual screenings have demonstrated the ability of prioritizing equally well agonists and blockers of the receptor over non-binders. Since these docking experiments were performed with a rigid representation of the receptor, their results are likely to reflect the initial binding of the agonists, prior to the sequence of conformational changes that they induce to the receptor.<sup>26,27</sup>

The sensitivity of fluorinated NE analogues to the identity of residue 293 suggests that the C–F bond is oriented towards that

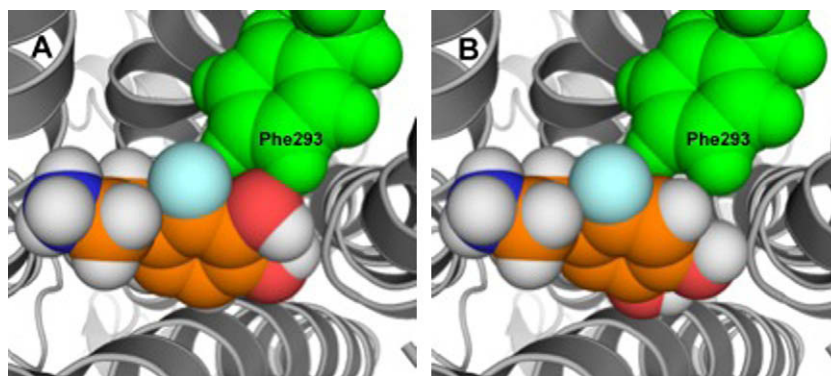


**Figure 3.** The binding modes of 2FNE and 6FNE at the N293F mutant  $\beta_2$ -adrenergic receptor. Although the binding orientations of the catechol rings stay the same for each ligand in the N293F mutant receptor, the added bulk of the F293 side chain sterically clashes with the hydroxyl groups of 2FNE (A), but not 6FNE (B). This unfavorable interaction is predicted to cause the reduced affinity of 2FNE for the mutant receptor. New hydrophobic interactions are likely to be responsible for the gain of affinity of 6FNE for the N293F mutant receptor.

position, as supported by additional modeling and docking studies. Although NE, 2FNE, and 6FNE have similar binding modes, the aromatic rings of NE and 2FNE have *meta*-hydroxyl groups that point toward the extracellular region, whereas the catechol ring of 6FNE binds in the opposite orientation to promote identical placement of the fluorine substituent. The presence of the bulky phenylalanine side chain in the N293F mutant causes a steric clash with the *meta*-hydroxyl group of NE and 2FNE, but not 6FNE, which instead benefits from the addition of favorable aromatic and hydrophobic interactions.

The affinities of the remaining N293 mutant receptors can be explained in a similar manner. The N293A mutant has the lowest affinity for every ligand due to the lack of any favorable contacts and hydrogen bonds that were present in the wild type receptor, while not adding any hydrophobic or aromatic contacts that would help to increase affinity. Mutating N293 to leucine adds favorable hydrophobic interactions, but it eliminates any potential hydrogen bonds found in the wild type receptor. Finally, the N293Q mutant, while offering the same positive charge as the wild type asparagine side chain, also contains a longer side chain, resulting in steric clashes that reduce each ligand's affinity. These observations provide a possible explanation for the selectivity of the  $\beta_2$ -adrenergic receptor toward 2FNE.

## 4. Experimental section

### 4.1. Site-directed mutagenesis

The human  $\alpha_{1b}$ - and  $\beta_2$ -adrenergic receptor sequences in the pcDNA3.1(+) vector were obtained from the UMR cDNA Resource Center. Point mutations were introduced into the receptors by polymerase chain reaction (QuikChange site-directed mutagenesis strategy, Stratagene) as per manufacturer's instructions. Mutations were confirmed by DNA sequencing.

### 4.2. Transient expression of receptor constructs

COS7 cells were grown in DMEM (Invitrogen), supplemented with 10% fetal bovine serum, 2 mM L-glutamine, 100 units/mL penicillin and 100  $\mu$ g/mL streptomycin at 37 °C in a humidified 5% CO<sub>2</sub> incubator. Approximately 24 h prior to transfection,  $1 \times 10^6$  cells were seeded in 100 mm plates. Transfection of cells was accomplished with plasmid DNAs (4  $\mu$ g of total DNA per 100 mm dish) using Lipofectamine and Plus reagent as per manufacturer's instructions (Invitrogen). Cells were harvested 48 h after transfection for receptor binding studies.

### 4.3. Receptor binding assays

Approximately 48 h after transfection, COS7 cells were washed with ice-cold PBS, scraped off the dishes in cold binding buffer (50 mM Tris, 1 mM EDTA, pH 7.5) and homogenized in binding buffer using a Polytron tissue homogenizer. Cell membranes were collected by centrifugation at 20,000g at 4 °C for 15 min and homogenized as before. Aliquots were stored at –80 °C until use. Protein concentrations of the membrane preparations were determined using the Pierce BCA Protein Assay kit with bovine serum albumin as the standard. Radioligand binding studies were carried out with membrane homogenates from COS7 cells (25  $\mu$ g protein per tube). Reaction mixtures were incubated for 1 h at 25 °C in a 500  $\mu$ L final volume of binding buffer. In saturation binding assays with the  $\beta_2$ -adrenergic receptor (wild type and mutants), six different concentrations of [<sup>3</sup>H]-dihydroalprenolol (DHA) (Perkin–Elmer, specific activity 117.8 Ci/mmol), ranging from 0.5 to 10 nM were tested. In competition binding assays, incubations were carried out with 0.5 nM [<sup>3</sup>H]DHA in the presence of 6 different concentrations of the NE, 6FNE, or 2FNE (1 nM to 1 mM). Nonspecific binding was assessed in the presence of 1  $\mu$ M propranolol. For the  $\alpha_{1b}$ -adrenergic receptor, [<sup>3</sup>H]-prazosin (Perkin–Elmer, specific activity 85.0 Ci/mmol), ranging from 0.1 to 10 nM were tested. In competition binding assays, incubations were carried out with 0.5 nM [<sup>3</sup>H]-prazosin in the presence of six different concentrations of NE, 6FNE, or 2FNE (1 nM to 1 mM). Nonspecific binding was assessed in the presence of 1  $\mu$ M prazosin. For both receptor subtypes bound and free ligand were separated by vacuum filtration over GF/B filters (Whatman), pretreated with 0.3% polyethyleneimine for 3 h. The filters were washed thrice with 5 mL of ice-cold water, dried, and placed in vials with 7 mL of Biosafe II scintillation mixture (RPI Corp.). Radioactivity bound to the filters was determined after 18 h of extraction. All data from saturation and inhibition assays were analyzed using GraphPad Prism 4.0.

### 4.4. Computational methods

In the initial phase of this work, the site-directed mutagenesis experiments were designed through a rhodopsin-based homology model of the  $\beta_2$ -adrenergic receptor. The details on the construction of this model and its structural features have been described elsewhere.<sup>13</sup> For the rest of the study, the modeling was based on the crystal structure of the  $\beta_2$ -adrenergic receptor in complex with carazolol (PDB ID: 2rh1),<sup>19,20</sup> and was carried out with the Schrödinger package, SUITE 2008.<sup>23</sup> The crystal structure of the  $\beta_2$ -adrenergic receptor was preprocessed with the Protein Preparation

Workflow in the MAESTRO user interface of the Schrödinger package. This added hydrogens, which were subsequently minimized using the OPLS\_2001 force field and *impact* molecular mechanics engine while heavy atoms were constrained, and it also optimized the protonation state of histidine residues and the orientation of hydroxyl groups, asparagine residues, and glutamine residues. For the mutant receptor, N293 was mutated to phenylalanine using the Mutate Residue option in MAESTRO, and the side chain was subsequently minimized using a truncated-Newton method and the OPLS\_2008 force field, treating solvation with the SGB continuum solvation model. The compounds were automatically docked into the crystallized  $\beta$ 2-adrenergic receptor binding site by means of GLIDE XP 5.0.<sup>22</sup> In the receptor grid generation, no scaling factors were applied to the van der Waals radii of the receptor's atoms. The docked ligand was confined to a box centered on Val114, with a size capable of accommodating ligands with a length  $\leq 15$  Å, and with a box of 10 Å for the ligand diameter midpoint. The scaling factor for the van der Waals radii of the docked ligand was set to 0.80, with a partial charge cutoff of 0.15e. The maximum number of poses to pass the initial phase of the GLIDE screen and move onto the refinement phase was set to 5000, however poses outside of a window of 100 kcal/mol from the lowest energy pose were discarded; the maximum number of poses to pass the refinement phase and move onto the grid-based energy minimization phase was set to 800—for this phase, the distance dependent dielectric constant was set to 2.0 and maximum number of conjugate gradient steps was set to 100; ligand poses with Coulomb-vdW energy greater than 0.0 kcal/mol were rejected; ligand poses with a root mean square deviation lower than 0.5 Å or a maximum atomic displacement lower than 1.3 Å were discarded as duplicate; the maximum number of top scoring poses to be subjected to a final full force field post-docking minimization was set to 10; the maximum number of top scoring poses to be recorded in the output was set to 3.

### Acknowledgment

This research was supported by the intramural research funds of NIDDK.

### References and notes

- Perez, D. M. In *The Adrenergic Receptors: in the 21st Century*; Totowa, N. J., Ed.; Humana Press, 2006.
- Alquist, R. P. *Am. J. Physiol.* **1948**, 153, 586.
- (a) Bylund, D. B.; Eikenberg, D. C.; Hieble, J. P.; Langer, S. Z.; Lefkowitz, R. J.; Minneman, K. P.; Molinoff, P. B.; Ruffolo, R. R., Jr.; Trendelenburg, A. U. *Pharmacol. Rev.* **1994**, 46, 121; (b) Bylund, D. B. *Trends Pharmacol. Sci.* **1988**, 9, 356.
- Cantacuzene, D.; Kirk, K. L.; McCulloh, D. H.; Creveling, C. R. *Science* **1979**, 204, 1217.
- Kirk, K. L.; Cantacuzene, D.; Nimitkitpaisan, Y.; McCulloh, D.; Padgett, W. L.; Daly, J. W.; Creveling, C. R. *J. Med. Chem.* **1979**, 22, 1493.
- Olsen, J.; Banner, D. W.; Seiler, P.; Tschopp, T.; Obst-Sander, U.; Kansy, M.; Müller, K.; Diedrich, F. A. *ChemBioChem* **2004**, 5, 666.
- Kirk, K. L. *J. Fluorine Chem.* **1995**, 72, 261.
- Kirk, K. L.; Olubajo, O.; Buchhold, K.; Lewandowski, G.; Gusovsky, F.; McCulloh, D.; Daly, J. W.; Creveling, C. R. *J. Med. Chem.* **1986**, 29, 1982.
- Adejare, A.; Nie, J.-Y.; Hebel, D.; Brackett, L. E.; Choi, O.; Gusovsky, F.; Padgett, W.; Daly, J. W.; Creveling, C. R.; Kirk, K. L. *J. Med. Chem.* **1991**, 34, 1063.
- Chen, B.-H.; Padgett, W. L.; Gusovsky, F.; Creveling, C. R.; Daly, J. W.; Kirk, K. L. *Med. Chem. Res.* **1992**, 2, 342.
- Calderon, S.; Gusovsky, F.; Garraffo, H. M.; Creveling, C. R.; Daly, J. W.; Nie, J.-Y.; Furlano, D. C.; Kirk, K. L. *Med. Chem. Res.* **1992**, 2, 419.
- Nimit, Y.; Cantacuzene, D.; Kirk, K. L.; Creveling, C. R.; Daly, J. W. *Life Sci.* **1980**, 27, 1577.
- Costanzi, S. *J. Med. Chem.* **2008**, 51, 2907.
- Strader, C.; Fong, T.; Tota, M.; Underwood, D.; Dixon, R. *Annu. Rev. Biochem.* **1994**, 63, 101.
- Sato, T.; Kobayashi, H.; Nagao, T.; Kurose, H. *Br. J. Pharmacol.* **1999**, 128, 272.
- Swaminath, G.; Xiang, Y.; Lee, T.; Steenhuis, J.; Parnot, C.; Kobilka, B. *J. Biol. Chem.* **2004**, 279, 686.
- Freddolino, P.; Kalani, M.; Vaidehi, N.; Floriano, W.; Hall, S.; Trabanino, R.; Kam, V.; Goddard, W. A., III *Proc. Natl. Acad. Sci. U.S.A.* **2004**, 101, 2736.
- Xhaard, H.; Rantanen, V.; Nyrönen, T.; Johnson, M. *J. Med. Chem.* **2006**, 49, 1706.
- Rosenbaum, D. M.; Cherezov, V.; Hanson, M. A.; Rasmussen, S. G.; Thian, F. S.; Kobilka, T. S.; Choi, H. J.; Yao, X. J.; Weis, W. I.; Stevens, R. C.; Kobilka, B. K. *Science* **2007**, 318, 1266.
- Cherezov, V.; Rosenbaum, D. M.; Hanson, M. A.; Rasmussen, S. G. F.; Thian, F. S.; Kobilka, T. S.; Choi, H.; Kuhn, P.; Weis, W. I.; Kobilka, B. K.; Stevens, R. C. *Science* **2007**, 318, 1258.
- Kirk, K. L.; Creveling, C. R. *Med. Chem. Rev.* **1984**, 4, 189.
- GLIDE, version 5.0, Schrödinger, LLC, New York, NY, 2008.
- MAESTRO, version 8.5, Schrödinger, LLC, New York, NY, 2008.
- Yao, X.; Parnot, C.; Deupi, X.; Ratnala, V. R.; Swaminath, G.; Farrens, D.; Kobilka, B. *Nat. Chem. Biol.* **2006**, 2, 417.
- Kobilka, B. K.; Deupi, X. *Trends Pharmacol. Sci.* **2007**, 28, 397.
- De Graaf, C.; Rognan, D. *J. Med. Chem.* **2008**, 51, 4978.
- Vilar, S.; Karpiak, J.; Costanzi, S. *J. Comput. Chem.* **2009**. doi:10.1002/jcc.21346.